Inorg. Chem. **2003**, *42*, 6265–6273

Synthesis of a Single Four-Ring (S4R) Molecular Zinc Phosphate and Its Assembly to an Extended Polymeric Structure: A Single-Crystal and in-Situ MAS NMR Investigation

Srinivasan Natarajan,*,†,‡ Leo van Wullen,‡ Wilhelm Klein,‡ and Martin Jansen*,‡

Framework Solids Laboratory, Chemistry and Physics of Materials Unit, Jawaharlal Nehru Centre for Advanced Scientific Research, Jakkur P.O., Bangalore 560 064, India, and Max-Planck-Institut für Festkörperforschung, Heisenbergstrasse 1, D-70569 Stuttgart, Germany

Received June 3, 2003

A reaction of ZnO, HCl, H_3PO_4, and 2-pyridylpiperazine in THF/H_2O mixture at 75 °C for 72 h produces a new zinc phosphate, $[(C_5NH_5)(C_4N_2H_{10})][Zn(H_2PO_4)_2(HPO_4)]$, **I**. Zinc phosphate **I** consists of single four-ring (S4R) units with terminal phosphoryl groups hanging from the Zn center. On reaction with zinc acetate dihydrate in the presence of water at 100 °C, **I** gave another new zinc phosphate, $[(C_5NH_5)(C_4N_2H_{10})][Zn_2(H_2PO_4)(HPO_4)(PO_4)]\cdot 2H_2O$, **II**. **II** has a layer structure with apertures formed by 4- and 8-T atoms (T = Zn, P). An examination of the two structures reveals that **I** and **II** are related, **II** being formed by the direct addition of Zn^{2+} ions to **I**. Room-temperature ^{31}P MAS NMR studies show the presence of different phosphorus species in both compounds. An in-situ ^{31}P MAS NMR investigation on the formation of **II** from **I** in the presence of Zn^{2+} ions and water reveals the transformation to be facile. What is noteworthy in this study is that the structural integrity of the S4Rs has been maintained during the formation of **II**. Donor–acceptor hydrogen bond interactions and π–π interactions involving the pyridyl groups also appear to play subtle roles in both phosphates. This study, the first attempt of its kind, combines the principles of supramolecular organic chemistry with inorganic building units and contributes to our understanding of the formation of framework solids.

Introduction

Solids possessing open-framework structures constitute an important branch of the family of inorganic compounds. After the seminal work of Wilson et al. on the synthesis of aluminum phosphates in 1982,[1] extensive investigations during the last two decades produced a large variety of new inorganic solids with unusual structural features.[2] The continuing interest is mainly due to the close structural relationships of some of these new phosphates to aluminosilicate minerals[3] and also to their potential applications in the areas of catalysis, sorption, and separation processes.[4] Of the many open-framework phosphates that have been prepared and characterized, those of zinc constitute an important family.[5−9] Thus, zinc phosphates with zero-,[5] one-,[6,7] two-,[8] and three-dimensionally extended[9] structures are known.

Despite the discovery of a large number of compounds with novel structures, our understanding of the formation of

* To whom correspondence should be adddressed. E-mail: raj@jncasr.ac.in (S.N.); m.jansen@fkf.mpg.de (M.J.).
† Jawaharlal Nehru Centre for Advanced Scientific Research.
‡ Max-Planck-Institut für Festkörperforschung.

(1) (a) Wilson, S. T.; Lok, B. M.; Flanigan, E. M. U.S. Patent 1982, 4 310 440. (b) Wilson, S. T.; Lok, B. M.; Messina, C. A.; Cannan, T. R.; Flanigan, E. M. *J. Am. Chem. Soc*. **1982**, *104*, 1146.
(2) Cheetham, A. K.; Ferey, G.; Loiseau, T. *Angew. Chem., Int. Ed*. **1999**, *39*, 3268 and references therein.
(3) Baerlocher, C., Meier, W. M., Olson, D. H., Eds. *Atlas of zeolitic structure types*; Elsevier: London, 2001.
(4) (a) Thomas, J. M.; Raja, R.; Sankar, G.; Bell, R. G. *Acc. Chem. Res*. **2001**, *34*, 191 and the references therein. (b) Thomas, J. M. *Top. Catal*. **2001**, *15*, 85. (c) Thomas, J. M.; Raja, R. *Aust. J. Chem*. **2001**, *54*, 551.
(5) (a) Neeraj, S.; Natarajan; S., Rao, C. N. R. *J. Solid State Chem*. **2000**, *150*, 417. (b) Ayi, A. A.; Choudhury, A.; Natarajan, S.; Neeraj, S.; Rao, C. N. R. *J. Mater. Chem*. **2001**, *11*, 1181. (c) Harrison, W. T. A.; Hanooman, L. *J. Solid State Chem*. **1997**, *131*, 363.
(6) (a) Chavaz, A. V.; Nenoff, T. M.; Hanooman, L.; Harrison, W. T. A. *J. Solid State Chem*. **1999**, *147*, 584. (b) Chidambaram, D.; Neeraj, S.; Natarajan, S.; Rao, C. N. R. *J. Solid State Chem*. **1999**, *147*, 154. (c) Reinert, P.; Zabukovec, N.; Patarin, J.; Kaucic, V. *Eur. J. Solid State Inorg. Chem*. **1998**, *136*, 373. (d) Harrison, W. T. A.; Bircsak, Z.; Hanooman, L.; Zhang, Z. J. *J. Solid State Chem*. **1998**, *136*, 93. (e) Ayi, A. A.; Neeraj, S.; Choudhury, A.; Natarajan, S.; Rao, C. N. R. *J. Phys. Chem. Solids* **2001**, *62*, 1481.
(7) Rao, C. N. R.; Natarajan, S.; Neeraj, S. *J. Am. Chem. Soc*. **2000**, *122*, 2810.

10.1021/ic0301831 CCC: $25.00
Published on Web 09/06/2003

these phases continues to be poor. The difficulty in obtaining information related to the mechanism(s) is partly because the materials are, generally, prepared under hydrothermal conditions, the hydrothermal reaction vessel being the proverbial black box. There have, however, been some suggestions with regard to the role of the amine in the formation of these structures and to the secondary building units.[10]

Recently, there has been a growing interest in the construction of solids with extended structures from molecular building blocks due to the principal advantages it offers for the design of materials. The appealing concepts of employing discrete molecular building units for the assembly of extended networks, however, requires careful isolation and stabilization of such building units. Supramolecular organization of organic compounds from molecular building units has developed to maturity in the past few years.[11] Supramolecular inorganic chemistry, on the other hand, is at a nascent stage. The concepts of supramolecular inorganic chemistry have been shown elegantly in the large scale assembly of polyoxometalates.[12] The challenge one faces in supramolecular inorganic chemistry is to establish the presence of building units and, if so, whether one can demonstrate how they are involved in the formation of larger structures. In the area of open-framework solids, design and control of the formation constitute an important facet of the research.[13,14] While it is desirable to synthesize large number of materials with new structures, it is also important to understand the role of the building units and the reaction pathways involved in the formation of these solids.

We have been aiming to combine the principles of supramolecular organic chemistry with inorganic building units to form new solids. During the course of such investigations, we have now synthesized a new zinc phosphate, $[(C_5NH_5)(C_4N_2H_{10})][Zn(H_2PO_4)_2(HPO_4)]$, **I**, consisting of an independent single four-ring (S4R) unit, in the presence of 2-pyridylpiperazine (Py-Pip). S4Rs are the fundamental building unit in many of the aluminosilicate zeolites and aluminophosphates.[3] This S4R zinc phosphate, **I**, readily reacts with Zn^{2+} ions to give rise to a layered structure, $[(C_5NH_5)(C_4N_2H_{10})][Zn_2(H_2PO_4)(HPO_4)(PO_4)]\cdot 2H_2O$, **II**. It is proposed that the formation of **II** is established via the linkage of S4R units by Zn^{2+} cations, resulting in an extended 2D open framework. This is the first example, to our knowledge, of the use of a fundamental building unit and its direct assembly into an extended structure within the family of inorganic framework solids. It appears that 2-pyridylpiperazine, employed during the synthesis of **I**, may have played a subtle role in the assembly, as the $\pi-\pi$ interactions between the pyridine molecule presumably control the organization of the S4R into an extended architecture. The synthesis of **I**, and its transformation to **II**, in a way, is reminiscent of the control achieved by organic supramolecular crystal engineering employing the $\pi-\pi$ interactions. We have carried out MAS NMR investigations on **I** and **II**, and also to understand the formation of **II** from **I**, we have performed in-situ MAS NMR studies. In this paper the synthesis, structure, and MAS NMR investigations of the two phases and their intricate relationships are presented.

Experimental Section

Synthesis and Initial Characterization. Compound **I** was synthesized in the presence of 2-pyridylpiperazine (Py-Pip). In a typical experiment, 0.15 g of ZnO was dispersed in a mixture of 2 mL of THF and 1 mL of water. To this, 0.36 mL of HCl (35%), 0.4 mL of H_3PO_4 (85%), and 0.15 mL of glacial acetic acid were added under continuous stirring. Finally, 0.6 mL of Py-Pip was added to the above, resulting in a polymeric precipitate. The mixture with the composition 1:2:3:2:1 $ZnO-HCl-H_3PO_4-$Py-Pip$-CH_3COOH$ in 20:67 $THF-H_2O$ was transferred into a PTFE-lined stainless steel autoclave (15 mL) and heated at 75 °C for 72 h. The initial pH of the mixture was ~6, and the pH after the reaction was ~5. The resulting product, a crop of rod-shaped colorless crystals, was filtered out under vacuum and dried at ambient temperature. The synthesis, when carried out at 100 °C, results in an identical product but with poorer quality of crystals. The only solid product from these reactions was **I** with a yield of ~80% based on

(8) (a) Neeraj, S.; Natarajan, S.; Rao, C. N. R. *Chem. Mater*. **1999**, *11*, 1390. (b) Liu, Y. L.; Liu, W.; Xing, Y.; Shi, Z.; Fu, Y. L.; Pang, W. Q. *J. Solid State Chem*. **2002**, *166*, 265. (c) Xing, Y.; Liu, Y. L.; Shi, Z.; Zhang, P.; Fu, Y. L.; Cheng, C.; Pang, W. Q. *J. Solid State Chem*. **2002**, *163*, 364. (d) Chiang, Y. P.; Kao, H. M.; Lii, K. H. *J. Solid State Chem*. **2001**, *162*, 168. (e) Wiebcke, M. *J. Mater. Chem*. **2002**, *12*, 143. (f) Yao, Y. W.; Cui, A. L. *Chem. Lett*. **2001**, 1148. (g) Liu, W.; Liu, Y. L.; Shi, Z.; Pang, W. Q. *J. Mater. Chem*. **2000**, *10*, 1451. (h) Neeraj, S.; Natarajan, S. *Int. J. Inorg. Mater*. **1999**, *1*, 317. (i) Neeraj, S.; Natarajan, S. *Cryst. Growth Des.* **2001**, *1*, 491. (j) Choudhury, A.; Natarajan, S.; Rao, C. N. R. *J. Solid State Chem*. **2001**, *157*, 110. (k) Harrison, W. T. A.; Phillips, M. L. F.; Clegg, W.; Teat, S. J. *J. Solid State Chem*. **1999**, *148*, 433 and references therein.

(9) (a) Feng, P.; Bu, X.; Stucky, G. D. *Angew. Chem., Int. Ed. Engl*. **1995**, *34*, 1745. (b) Gier, T. E.; Stucky, G. D. *Nature* **1991**, *349*, 508. (c) Ng, H. Y.; Harrison, W. T. A. *Microporous Mesoporous Mater*. **2001**, *50*, 187. (d) Nenoff, T. M.; Harrison, W. T. A.; Gier, T. E.; Stucky, G. D. *J. Am. Chem. Soc*. **1991**, *113*, 78. (e) Yang, G.-Y.; Sevov, S. C. *J. Am. Chem. Soc*. **1999**, *121*, 8389. (f) Simon, A.; Josien, L.; Gramlich, V.; Patarin, J. *Microporous Mesoporous Mater*. **2001**, *47*, 135. (g) Yu, J. H.; Wang, Y.; Shi, Z.; Xu, R. R. *Chem. Mater*. **2001**, *13*, 2972. (h) Rodgers, J. A.; Harrison, W. T. A. *J. Mater. Chem*. **2000**, *10*, 2853. (i) Kongshaug, K. O.; Fjellvag, H.; Lillerud, K. P. *Micorporous Mesoporous Mater*. **2000**, *39*, 341. (j) Liu, Y.; Na, L.; Zhu, G.; Xio, F.-S.; Pang, W.; Xu, R. *J. Solid State Chem*. **2000**, *149*, 107. (k) Harrison, W. T. A.; Martin, T. E.; Gier, T. E.; Stucky, G. D. *J. Mater. Chem*. **1992**, *2*, 1127. (l) Bu, X.; Feng, P.; Gier, T. E.; Stucky, G. D. *Zeolites* **1997**, *19*, 2000. (m) Harrison, W. T. A.; Nenoff, T. M.; Gier, T. E.; Stucky, G. D. *Inorg. Chem*. **1992**, *31*, 5395. (n) Feng, P.; Bu, X.; Stucky, G. D. *J. Solid State Chem*. **1996**, *125*, 243. (o) Bu, X.; Feng, P.; Gier, T. E.; Stucky, G. D. *Zeolites* **1997**, *19*, 2000. (p) Broach, R. W.; Bedard, R. L.; Song, S. G.; Pluth, J. J.; Bram, A.; Riekel, C.; Weber, H.-P. *Chem. Mater*. **1999**, *11*, 2076. (q) Harrison, W. T. A.; Philips, M. L. F. *Chem. Mater*. **1997**, *9*, 1837. (r) Harrison, W. T. A.; Hannooman, L. *Angew. Chem., Int. Ed. Engl*. **1997**, *36*, 640. (s) Kongshaug, K. O.; Fjellvag, H.; Lillerud, K. P. *J. Mater. Chem*. **1999**, *9*, 3119. (t) Chidambaram, D.; Natarajan, S. *Mater. Res. Bull*. **1998**, *33*, 1275. (u) Neeraj, S.; Natarajan, S.; Rao, C. N. R. *Chem. Commun*. **1999**, 165. (v) Choudhury, A.; Natarajan, S.; Rao, C. N. R. *Inorg. Chem*. **2000**, *39*, 4295. (w) Neeraj, S.; Natarajan, S. *Chem. Mater*. **2000**, *11*, 2735.

(10) (a) Davis, M. E.; Lobo, R. F. *Chem. Mater*. **1992**, *4*, 756. (b) Ferey, G. *J. Solid State Chem*. **2000**, *152*, 37.

(11) Lehn, J. M., Ed. *Supramolecular Chemistry, Concepts and Perspectives*; VCH: Weinheim, Germany, 1995.

(12) Müller, A.; Reuter, H.; Dillinger, S. *Angew. Chem., Int. Ed. Engl*. **1995**, *34*, 2328.

(13) (a) Francis, R. J.; O'Brain, S.; Fogg, A. M.; Halasyamani, P. S.; O'Hare, D.; Loiseau, T.; Ferey, G. *J. Am. Chem. Soc*. **1999**, *121*, 1002. (b) Walton, R. I.; Millange, F.; Le Bail, A.; Loiseau, T.; Serre, C.; O'Hare, D.; Ferey, G. *Chem. Commun*. **2000**, 203. (c) Walton, R. I.; Loiseau, T.; O'Hare, D.; Ferey, G. *Chem. Mater*. **2000**, *12*, 1977. (d) Walton, R. I.; Norquist, A. J.; Neeraj, S.; Natarajan, S.; Rao, C. N. R.; O'Hare, D. *Chem. Commun*. **2001**, 1990 and the references therein.

(14) Rao, C. N. R.; Natarajan, S.; Choudhury, A.; Neeraj, S.; Ayi, A. A. *Acc. Chem. Res*. **2001**, *34*, 80.

ZnO. **II** was prepared under hydrothermal conditions by heating equal moles of **I** and zinc acetate, $[Zn(OAc)_2 \cdot 2H_2O]$, in a 7 mL pressure vessel with 1 mL of water at 180 °C for 24 h. From this reaction plates of good quality resulted, and the yield is nearly 100%. In a separate experiment, a mixture of the composition 1:2:2:2:1 ZnO−HCl−H_3PO_4−Py-Pip−CH_3COOH in 20:67 THF−H_2O was prepared, as above, and heated at 75 °C for 72 h followed by at 150 °C for 24 h resulting in a pure phase of **II**. The initial pH of the mixture was ∼7, and the pH after the reaction did not show appreciable change. Our efforts to prepare **I** and **II** in pure aqueous medium, however, were not successful. The role of acetic acid in the synthesis mixture is still not clear. An EDAX analysis on many single crystals indicated a Zn:P ratio of 1:3 and 2:3 for **I** and **II**, respectively. Elemental analysis results of the bulk product are also consistent with the stoichiometry. Anal. Found for **I**: C, 21.18; H, 3.92; N, 8.54. Calcd for **I**: C, 20.81; H, 3.66; N, 8.08. Found for **II**: C, 18.1; H, 3.76; N, 6.59. Calcd for **II**: C, 17.45; H, 3.39; N, 6.79.

The initial characterization was carried out using powder X-ray diffraction (XRD), thermogravimetric analysis (TGA), and infrared spectroscopy. The powder XRD pattern confirmed that the products were new materials; the patterns were entirely consistent with the structures determined using the single-crystal X-ray diffraction. A least-squares fit of the powder XRD (Cu Kα radiation) lines, using the *hkl* indices generated from single-crystal X-ray data, resulted in the following cell parameters. **I**: $a = 8.1652(7)$, $b = 8.3888(7)$, $c = 14.2669(14)$ Å; $\alpha = 73.190(7)$, $\beta = 87.51(8)$, $\gamma = 78.488(8)°$. **II**: $a = 8.7133(6)$, $b = 10.0329(7)$, $c = 12.1257(10)$ Å; $\alpha = 93.365(7)$, $\beta = 100.972(6)$, $\gamma = 98.537(7)°$. These values are in reasonable agreement with those determined using the single-crystal XRD.

Thermogravimetric analyses (TGA) of compounds **I** and **II** were carried out in oxygen atmosphere (flow rate = 50 mL min^{-1}) in the range between 25 and 700 °C (heating rate = 5 °C min^{-1}), employing alumina crucibles. For **I**, the release of amine from the structure was observed to be too exothermic to allow for a reliable measurement. For **II**, the studies indicate that the weight loss occurs in two steps followed by a long tail. The total observed weight loss of 36% corresponds well with the loss of extraframework water and the amine molecule and the condensation of the phosphates (calcd 37.8%). The loss of the amine molecule resulted in the collapse of the framework structure, leading to the formation of largely amorphous weakly diffracting material (XRD) that corresponds to a dense zinc phosphate phase: $Zn_2P_2O_7$ (JCPDS: 34-1275).

Infrared (IR) spectra as KBr pellets of **I** and **II** were recorded in the range 400−4000 cm^{-1}. The spectra showed typical peaks, with little differences between the spectra. Peaks corresponding to the various stretching and bending vibrations have been observed: $\nu(HPO_4) = 1090$ cm^{-1} (m), $\nu(H_2PO_4) = 918$ cm^{-1} (s) and 1141 cm^{-1} (m), $\nu(PO_4) = 1013$ cm^{-1} (s) (for **II**); $\nu(C_5H_5N^+) = 1540$−1640 cm^{-1} (s), $\delta(C_5H_5N^+) = 989$ cm^{-1} (w) and 748 cm^{-1} (s), $\nu(CH_2) = 2912$ cm^{-1} (s), $\delta(CH_2) = 1463$ and 1444 cm^{-1} (m), $\nu(NH_2^+) = 2418$ and 2601 cm^{-1} (m), $\delta(NH_2^+) = 1419$ cm^{-1} (m), $\nu(C-C) = 1058$ cm^{-1} (s), $\nu(C=C) = 1543$ cm^{-1} (m). A strong band at 3600 cm^{-1} has been observed for **II**, corresponding to the extraframework water molecule.

Single-Crystal Structure Determination. A suitable colorless single crystal of each compound (0.20 × 0.20 × 0.32 mm for **I** and 0.24 × 0.24 × 0.12 mm for **II**) was carefully selected under a polarizing microscope and glued to a thin glass fiber with cyanoacrylate (superglue) adhesive. Crystal structure determination by X-ray diffraction was performed on a Siemens SMART-CCD diffractometer equipped with a normal focus, 2.4 kW sealed tube X-ray source (Mo Kα radiation, $\lambda = 0.710\ 73$ Å) operating at 50 kV and 40 mA. A hemisphere of intensity data was collected at room temperature in 1321 frames with ω scans (width of 0.30° and exposure time of 10 s/frame) in the 2θ range 3−46.5°. Pertinent experimental details for the structure determination of **I** and **II** are presented in Table 1. An absorption correction was applied using the SADABS program.[15] Other effects, such as absorption by the glass fiber, were simultaneously corrected. The structures were solved by direct methods using SHELXTL-PLUS,[16] and in each case, a sufficient fragment of the structure was revealed (Zn, P, and O) to enable the remainder of the non-hydrogen atoms to be located from difference Fourier maps and the refinements to proceed to R < 10%. All the hydrogen positions for **I** and **II** were initially located in the difference map, and for the final refinement the hydrogen atoms were placed geometrically and held in the riding mode. The last cycles of refinement included atomic positions for all atoms, anisotropic thermal parameters for all non-hydrogen atoms, isotropic thermal parameters for all hydrogen atoms, and, for the monomer, occupation factors for the two positions of the disordered H_2PO_4 residue. Full-matrix least-squares refinement against $|F^2|$ was carried out using the SHELXTL-PLUS[16] suite of programs. Details of the final refinement are given in Table 1. Selected bond distances and angles are given in Table 2 for **I** and in Table 3 for **II**.

Table 1. Crystal Data and Structure Refinement Parameters for **I**, $[(C_5NH_5)(C_4N_2H_{10})][Zn(H_2PO_4)_2(HPO_4)]$, and **II**, $[(C_5NH_5)(C_4N_2H_{10})][Zn_2(H_2PO_4)(HPO_4)(PO_4)] \cdot 2H_2O$

structure param	**I**	**II**
empirical formula	$C_9H_{20}N_3O_{12}P_3Zn$	$C_9H_{22}N_3O_{14}P_3Zn_2$
fw	520.56	619.94
T/K	293(2)	293(2)
space group	$P\bar{1}$ (No. 2)	$P\bar{1}$ (No. 2)
a/Å	8.139(2)	8.683(1)
b/Å	8.362(4)	9.997(1)
c/Å	14.202(3)	12.094(1)
α/deg	73.36(2)	93.341(1)
β/deg	87.56(2)	101.061(2)
γ/deg	78.31(3)	98.583(1)
V/Å^3	906.8(5)	1014.67(2)
Z	2	2
D_{calcd}/g cm^{-3}	1.906	2.029
μ/mm^{-1}	1.688	2.677
$R_1{}^a$ [$I > 2\sigma(I)$]	0.0315	0.0281
$wR_2{}^b$ [$I > 2\sigma(I)$]	0.0782	0.0686
$R_1{}^a$ (all data)	0.0378	0.0362
$wR_2{}^b$ (all data)	0.0809	0.0722

[a] $R_1 = \Sigma\,||F_o| - |F_c||/\Sigma|F_o|$. [b] $wR_2 = \{\Sigma[w(F_o^2 - F_c^2)^2]/\Sigma[w(F_o^2)^2]\}^{1/2}$. $w = 1/[\sigma^2(F_o)^2 + (aP)^2 + bP]$, $P = [\max(F_o^2,0) + 2(F_c)^2]/3$, where $a = 0.0394$ and $b = 0.4346$ for **I** and $a = 0.0354$ and $b = 0.4519$ for **II**.

Solid-State NMR Investigations. Solid-state nuclear magnetic resonance (NMR) experiments were performed on a Bruker DSX 400 spectrometer operating at 9.4 T with resonance frequencies of 162.0 and 400.13 MHz for ^{31}P and ^{1}H, respectively. A Bruker 4 mm CPMAS probe was used for all experiments. The ^{31}P MAS spectra were recorded using standard cross-polarization (CP) procedures and high power proton decoupling, employing magic angle spinning (MAS) frequencies between 1500 and 5000 Hz. In a typical experiment, rf fields of 62.5 kHz were used for ^{1}H and ^{31}P. Chemical shifts are reported relative to 85% H_3PO_4 as an external standard.

(15) Sheldrick, G. M. *SADABS Siemens area detector absorption correction program*; University of Göttingen: Göttingen, Germany, 1994.
(16) Sheldrick, G. M. *SHELXTL-PLUS A program for crystal structure solution and refinement*; University of Göttingen: Göttingen, Germany, 1997.

Table 2. Selected Bond Distances (Å) and Angles (deg) for **I**, $[(C_5NH_5)(C_4N_2H_{10})][Zn(H_2PO_4)_2(HPO_4)]$[a]

Zn(1)−O(1)	1.919(2)	P(2)−O(7)	1.555(3)
Zn(1)−O(2)	1.945(2)	P(2)−O(8)	1.561(3)
Zn(1)−O(5)	1.930(2)	P(3)−O(9)	1.504(3)
Zn(1)−O(9)	1.951(3)	P(3)−O(10)	1.509(3)
P(1)−O(1)	1.511(2)	P(3)−O(11)	1.542(3)
P(1)−O(2)$^{\#1}$	1.529(2)	P(3)−O(12)	1.560(3)
P(1)−O(3)	1.516(2)	P(3)−O(10a)	1.51(2)
P(1)−O(4)	1.572(3)	P(3)−O(11a)	1.55(2)
P(2)−O(5)	1.493(3)	P(3)−O(12a)	1.61(2)
P(2)−O(6)	1.518(3)		
O(1)−Zn(1)−O(2)	113.6(1)	O(7)−P(2)−O(8)	107.4(2)
O(1)−Zn(1)−O(5)	104.8(1)	O(9)−P(3)−O(10)	112.5(2)
O(1)−Zn(1)−O(9)	110.9(1)	O(9)−P(3)−O(11)	111.7(2)
O(2)−Zn(1)−O(5)	114.0(1)	O(9)−P(3)−O(12)	110.4(2)
O(2)−Zn(1)−O(9)	99.6(1)	O(10)−P(3)−O(11)	111.3(2)
O(5)−Zn(1)−O(9)	114.3(1)	O(10)−P(3)−O(12)	105.8(2)
O(1)−P(1)−O(2)$^{\#1}$	111.8(1)	O(11)−P(3)−O(12)	104.8(2)
O(1)−P(1)−O(3)	110.7(1)	O(9)−P(3)−O(10a)	123.0(7)
O(1)−P(1)−O(4)	105.7(2)	O(9)−P(3)−O(11a)	105.2(7)
O(2)$^{\#1}$−P(1)−O(3)	109.9(2)	O(9)−P(3)−O(12a)	110.0(8)
O(2)$^{\#1}$−P(1)−O(4)	108.1(1)	O(10a)−P(3)−O(11a)	108.1(11)
O(3)−P(1)−O(4)	110.5(1)	O(10a)−P(3)−O(12a)	106.4(11)
O(5)−P(2)−O(6)	115.8(2)	O(11a)−P(3)−O(12a)	102.2(11)
O(5)−P(2)−O(7)	110.8(2)	P(1)−O(1)−Zn(1)	128.1(1)
O(5)−P(2)−O(8)	106.3(2)	P(1)$^{\#1}$−O(2)−Zn(1)	134.7(2)
O(6)−P(2)−O(7)	106.5(2)	P(2)−O(5)−Zn(1)	149.8(2)
O(6)−P(2)−O(8)	109.8(2)	P(3)−O(9)−Zn(1)	135.7(2)

[a] Symmetry transformations used to generate equivalent atoms: #1, $-x$, $-y$, $-z$.

Table 3. Selected Bond Distances (Å) and Angles (deg) in **II**, $[(C_5NH_5)(C_4N_2H_{10})][Zn_2(H_2PO_4)(HPO_4)(PO_4)]\cdot 2H_2O$[a]

Zn(1)−O(1)$^{\#2}$	1.950(3)	P(1)−O(3)	1.508(3)
Zn(1)−O(3)	1.929(3)	P(1)−O(4)	1.576(3)
Zn(1)−O(5)	1.943(3)	P(2)−O(5)	1.516(3)
Zn(1)−O(9)$^{\#5}$	1.933(3)	P(2)−O(6)	1.520(3)
Zn(2)−O(2)$^{\#4}$	1.908(3)	P(2)−O(7)	1.535(3)
Zn(2)−O(6)$^{\#3}$	1.944(3)	P(2)−O(8)	1.542(3)
Zn(2)−O(8)	1.967(3)	P(3)−O(9)	1.512(3)
Zn(2)−O(10)	1.947(3)	P(3)−O(10)	1.502(3)
P(1)−O(1)	1.535(3)	P(3)−O(11)	1.547(3)
P(1)−O(2)	1.508(3)	P(3)−O(12)	1.568(3)
O(1)$^{\#2}$−Zn(1)−O(3)	108.1(1)	O(5)−P(2)−O(7)	110.2(1)
O(1)$^{\#2}$−Zn(1)−O(5)	104.5(1)	O(5)−P(2)−O(8)	107.7(2)
O(1)$^{\#2}$−Zn(1)−O(9)$^{\#5}$	118.7(1)	O(6)−P(2)−O(7)	110.2(2)
O(3)−Zn(1)−O(5)	102.3(1)	O(6)−P(2)−O(8)	108.8(1)
O(3)−Zn(1)−O(9)$^{\#5}$	108.8(1)	O(7)−P(2)−O(8)	108.7(2)
O(5)−Zn(1)−O(9)$^{\#5}$	113.3(1)	O(9)−P(3)−O(10)	114.5(2)
O(2)$^{\#4}$−Zn(2)−O(6)$^{\#3}$	118.4(1)	O(9)−P(3)−O(11)	111.7(2)
O(2)$^{\#4}$−Zn(2)−O(8)	107.3(1)	O(9)−P(3)−O(12)	105.3(2)
O(2)$^{\#4}$−Zn(2)−O(10)	120.3(1)	O(10)−P(3)−O(11)	109.5(2)
O(6)$^{\#3}$−Zn(2)−O(8)	113.3(1)	O(10)−P(3)−O(12)	111.0(2)
O(6)$^{\#3}$−Zn(2)−O(10)	97.8(1)	O(11)−P(3)−O(12)	104.5(1)
O(8)−Zn(2)−O(10)	98.1(1)	P(1)−O(1)−Zn(1)$^{\#2}$	134.2(2)
O(1)−P(1)−O(2)	111.9(2)	P(1)−O(2)−Zn(2)$^{\#4}$	141.7(2)
O(1)−P(1)−O(3)	112.3(2)	P(1)−O(3)−Zn(1)	134.4(2)
O(1)−P(1)−O(4)	106.5(2)	P(2)−O(5)−Zn(1)	140.3(2)
O(2)−P(1)−O(3)	111.6(2)	P(2)−O(6)−Zn(2)$^{\#3}$	134.5(2)
O(2)−P(1)−O(4)	109.9(2)	P(2)−O(8)−Zn(2)	122.2(1)
O(3)−P(1)−O(4)	104.1(1)	P(3)−O(9)−Zn(1)$^{\#1}$	131.6(2)
O(5)−P(2)−O(6)	111.2(2)	P(3)−O(10)−Zn(2)	133.1(2)

[a] Symmetry transformations used to generate equivalent atoms: #1, $x+1$, y, z; #2, $-x$, $-y+1$, $-z$; #3, $-x+1$, $-y$, $-z$; #4, $-x+1$, $-y+1$, $-z$; #5, $x-1$, y, z.

For the in-situ NMR experiments, a drop of distilled H_2O was added to an equimolar mixture of **I** and zinc acetate in the MAS rotor. Consecutive CP spectra were collected in 80 s each, the time interval, thus, defining the time resolution of our experiment.

Results

Structure of the Monomer, $[(C_5NH_5)(C_4N_2H_{10})][Zn(H_2PO_4)_2(HPO_4)]$, I. The asymmetric unit of **I** contains 27 non-hydrogen atoms. There are one Zn and three crystallographically distinct P atoms present in the asymmetric unit. The Zn atom is tetrahedrally coordinated by four oxygen atom neighbors, with average Zn−O bond lengths of 1.936 Å. The average O−Zn−O bond angles have the expected tetrahedral angle of 109.5°. The Zn atom is connected to four P atoms through Zn−O−P linkages, with an average bond angle of 137.1°. Of the three crystallographically independent P atoms, P(2) and P(3) are connected to Zn through one P−O−Zn linkage and have three terminal P−O bonds, and P(1) is connected to two different Zn atoms via two P−O−Zn linkages and possesses two terminal P−O bonds. One of the terminal PO_4 groups is positionally disordered through rotation around the P−O bond linked to the Zn atom. While O(9) and P(3) are fixed, two split positions for each O atom in a 8:1 ratio were found. Both split positions are fixed by hydrogen bonds to neighboring PO_4 groups; for the major present individual one more short H bond is found. The P−O distances longer than 1.54 Å are P−OH groups. This observation also corresponds well with the proton positions located in the difference Fourier maps. The P−O distances in the range 1.493−1.529 Å are P═O bonds. The marginally longer P═O are mainly due to the presence of a large number of hydrogen bond interactions in this compound. As expected, (ZnO)−P═O angles (average 114.8°) as well as the (ZnO)−P−(OZn) angle of 111.8° are significantly bigger than those O−P−O angles with an OH group involved therein (108.4°). O−P−O angles with two OH residues are again significantly smaller (104.8°). Selected bond distances and angles are listed in Table 2.

Zinc phosphate **I** is constructed by the vertex linking of ZnO_4, $PO_3(OH)$, and $PO_2(OH)_2$ tetrahedral units. The connectivity between these tetrahedral units gives rise to the fundamental building unit, the single four-ring (S4R) group. The S4Rs are made from two Zn and two P atoms connected via oxygen atoms. Each Zn center is linked to two terminal H_2PO_4 groups. The total negative charge on the four-membered ring monomer is balanced by the presence of one protonated Py-Pip molecule. S4R, with its terminal phosphate groups, is stabilized by extensive hydrogen bonding with other S4Rs as well as with amine molecules as shown in Figure 1. Thus, multipoint hydrogen bond interactions with short donor−acceptor (D−A) distances (2.52−2.80 Å) and nearly linear D−H···A angles of >150° are present in **I**. Both the terminal P−OH linkages and the hydrogen atoms of the amine molecules are involved in hydrogen bonding.

It has been shown that the terminal phosphoryl groups are generally reactive.[14] To enhance our understanding of the various pathways for the formation of these solids, it is important to keep the basic single four-ring (S4R) unit intact while carrying out investigations on the reactivity of the terminal P−OH groups. To achieve this, the S4R must be condensed, i.e., dephosphorylated, in the presence of just the

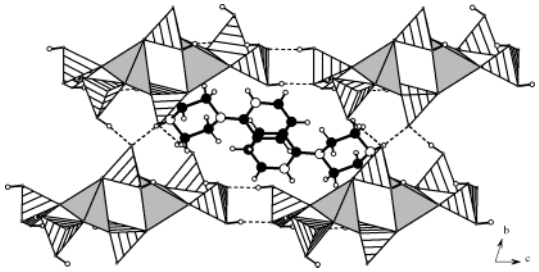

Figure 1. Structure of the S4R zinc phosphate, $[(C_5NH_5)(C_4N_2H_{10})][Zn(H_2PO_4)_2(HPO_4)]$, **I,** in the *bc* plane showing the arrangement of the S4Rs. Note the alignment of the Py-Pip molecule between the S4Rs. In the anionic part of the structure, PO_4 groups are drawn as white hatched tetrahedra and ZnO_4 as gray tretrahedra.

metal ion. We have performed such a reaction, resulting in the formation of **II**.

Structure of II, $[(C_5NH_5)(C_4N_2H_{10})][Zn_2(H_2PO_4)(HPO_4)(PO_4)]\cdot 2H_2O$. The asymmetric unit of **II** contains 31 nonhydrogen atoms, of which 17 belong to the framework, 12 belong to the guest amine molecule, and 2 belong to the extraframework water molecules. There are two crystallographically distinct Zn and three P atoms. The Zn atoms are tetrahedrally coordinated by their O atom neighbors with Zn−O bond lengths in the range 1.908(3)−1.967(3) Å (average Zn−O = 1.940 Å). The two zinc atoms are linked to four PO_4 groups with an average Zn−O−P angle of 134.0°. Of the three P atoms, P(1) and P(2) make three P−O−Zn linkages and possess one terminal P−O bond, and P(3) forms only two P−O−Zn connections with two terminal P−O bonds. The P−O distances are in the range 1.502(3)−1.576(3) Å (average 1.531 Å), and the O−P−O angles are in the range 104.1(2)−114.5(2)° (average 109.4°). These geometrical parameters are in good agreement with those reported for similar compounds in the literature.[5−9] The framework structure of $Zn_2(PO_4)_3$ would result in a net framework charge of −5. Three terminal P−O distances in the range of 1.547−1.576 Å are P−OH bonds and also correspond well with the proton positions located in the difference Fourier maps. The other terminal P(2)−O(7) distance of 1.535(3) Å is a P═O bond. The protonation of two of the nitrogen atoms of the amine molecule would ensure the complete charge balance in **II**. Selected bond distances and angles are presented in Table 3.

The zinc phosphate structure of **II** consists of ZnO_4, PO_4, $PO_3(OH)$, and $PO_2(OH)_2$ tetrahedral units vertex linked to give rise to an anionic extended two-dimensional layer structure. The fully protonated Py-Pip molecule is located between the layers. The most striking aspect of **II** is the layer architecture, formed by the direct condensation of the terminal phosphate groups of the S4R zinc phosphate with the Zn atoms. The view of the position of the amine and the layers are shown in Figure 2a. The layers, thus, are made only from four- and eight-membered apertures (Figure 2b). This is the first example, to our knowledge, of direct condensation of the single four-ring (S4R) unit in open-framework solids. The layers are stabilized by the hydrogen bond interactions between the framework oxygen atoms and the amine molecule. Important hydrogen bond interactions are listed in Table 4.

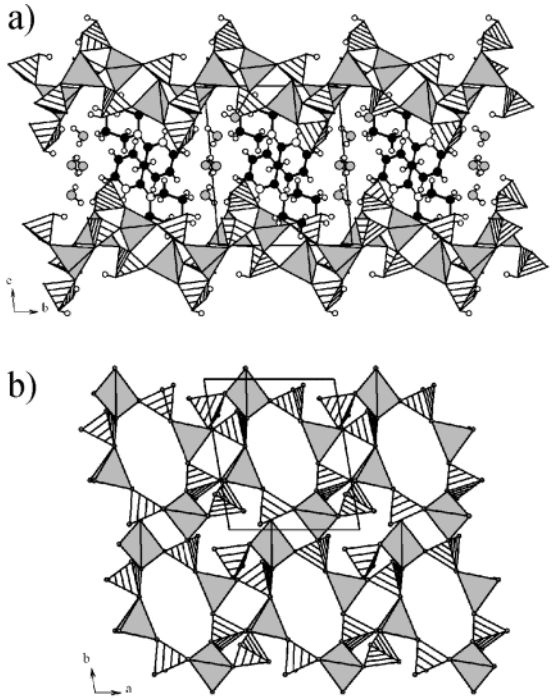

Figure 2. Structure of the layered zinc phosphate, $[(C_5NH_5)(C_4N_2H_{10})][Zn_2(H_2PO_4)(HPO_4)(PO_4)]\cdot 2H_2O$, **II**, (a) showing the arrangement of the layers in the *bc* plane and (b) in the *ab* plane showing a single layer. PO_4 groups are drawn as white hatched tetrahedra, ZnO_4 groups as gray tretrahedra.

Table 4. Important Hydrogen Bond Interactions in **I**, $[(C_5NH_5)(C_4N_2H_{10})][Zn(H_2PO_4)_2(HPO_4)]$, and **II**, $[(C_5NH_5)(C_4N_2H_{10})][Zn_2(H_2PO_4)(HPO_4)(PO_4)]\cdot 2H_2O$

D−H···moiety	D−H/Å	H···A/Å	D···A/Å	D−H···A/deg
		I		
N(3)−H(3b)···O(3)	0.90	1.93	2.729(2)	165.2
N(1)−H(1)···O(10a)	0.86	2.01	2.761(4)	145.9
N(3)−H(3a)···O(2)	0.90	1.85	2.795(4)	160.9
O(11)−H(11)···O(3)	0.82	1.71	2.524(3)	169.6
O(11)−H(11a)···O(3)	0.82	1.73	2.536(5)	161.9
O(7)−H(7)···O(10)	0.82	1.76	2.575(2)	170.5
O(12)−H(12)···O(6)	0.82	1.78	2.592(2)	168.4
O(4)−H(4)···O(10)	0.82	1.81	2.587(2)	159.0
O(8)−H(8)···O(6)	0.82	1.80	2.615(2)	172.0
		II		
N(3)−H(3b)···O(1)	0.90	1.87	2.774(3)	179.5
N(3)−H(3a)···O(6)	0.90	2.00	2.801(2)	148.2
N(1)−H(1)···O(8)	0.86	2.13	2.863(2)	142.5
O(11)−H(11)···O(7)	0.82	1.66	2.459(2)	166.1
O(4)−H(4)···O(7)	0.82	1.76	2.564(3)	168.3
O(12)−H(12)···O(14)	0.82	1.81	2.617(4)	166.5
O(14)−H(14b)···O(13)	0.87(3)	1.94	2.792(4)	163.7
O(13)−H(13a)···O(8)	0.90(3)	1.91	2.805(1)	177.1
O(14)−H(14a)···O(11)	0.84(3)	1.99	2.812(2)	164.5

Solid-State MAS NMR Studies. Room-temperature solid-state ^{31}P CP MAS NMR spectra for the monomer (S4R Zn phosphate), **I**, and the polymer (layered Zn phosphate), **II**, are presented in Figure 3a,b. In the spectrum of **I**, we find two signals at 3.9 and 3.1 ppm with a relative ratio of approximately 0.33 each and a signal at 0.8 ppm accompanied by a shoulder at 0.2 ppm, the combined areas of which amount to 0.33.

Each signal is accompanied by a set of spinning sidebands. The full spectrum (isotropic signal plus spinning sidebands)

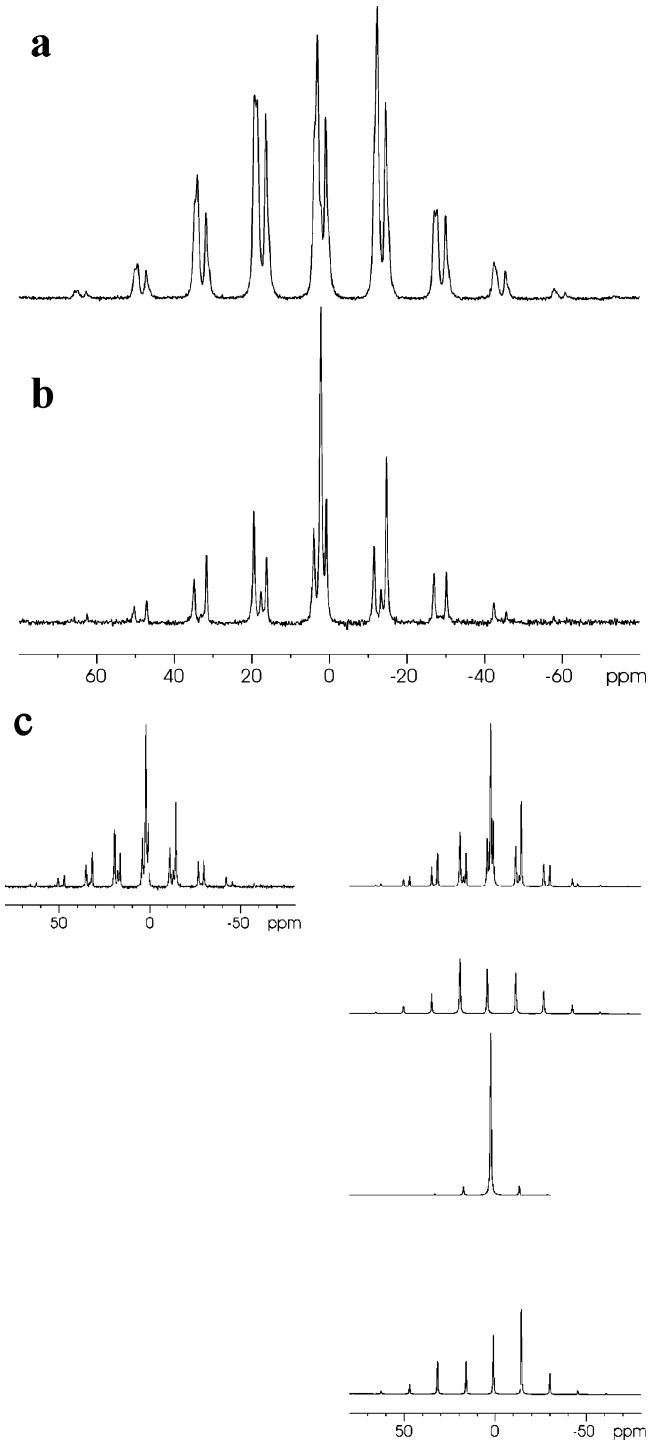

Figure 3. (a, b) ^{31}P-CPMAS NMR spectra of **I** and **II**. Experimental details: ν_{MAS}, 2500 Hz; contact time, 3 ms; ν_{RF}(^{1}H and ^{31}P), 62.5 kHz. (c) ^{31}P NMR spectrum of **II** (top left) together with the simulation (top right) and deconvolution into three individual components. The results of this procedure are compiled in Table 5.

was analyzed using the Bruker WinFit software to obtain total signal intensities and the full chemical shift (CS) tensor for the individual components. The data are compiled in Table 5.

The reason for the presence of four signals instead of the expected three (on the basis of the single-crystal data) is not clear. The probable reason for the splitting of the upfield signal is the presence of a small amount of water in the sample used for the NMR studies (vide infra).

Table 5. Compilation of Chemical Shift Data for the ^{31}P Signals in **I** and **II**

	δ_{iso}/ppm	Δ_{CS}/ppm	h	area/%
monomer (**I**)	3.9	−75	0.8	30
	3.1	66	0.6	34
	2.1	22	0.6	1[a]
	0.8	69	0.9	26[b]
	0.2	69	0.9	7[b]
polymer (**II**)	3.9	−74	0.8	33
	2.1	22	0.8	34
	0.7	74	0.4	33

[a] Impurity. [b] The combined areas of these two signals adds to 1/3 of the total area.

The ^{31}P CPMAS spectrum of **II** (Figure 3b) exhibits three different ^{31}P signals at 0.7, 2.1, and 3.9 ppm, each with a relative intensity of 0.33, in agreement with the results of the single crystal study. Figure 3c shows the simulation of the spectrum along with its deconvolution into three components; cf. Table 5.

Since the layered zinc phosphate, **II**, is obtained from the reaction of the S4R monomer, **I**, with zinc acetate in the presence of water, we followed the transformation of **I** into **II** using in-situ ^{31}P CPMAS experiments. A small amount of distilled H_2O (one drop) was added to an equimolar mixture of **I** and zinc acetate in the MAS rotor. Consecutive ^{31}P CPMAS spectra were acquired at room temperature within 80 s, starting approximately 2 min after H_2O addition. The in-situ spectra are presented in Figure 4. Interestingly, the observed splitting of the upfield signal disappears immediately upon addition of water.

In a comparison of the first and the last spectra of this series with the corresponding spectra of the monomer, **I** (Figure 3a), and the polymer, **II** (Figure 3b), it is clear that the reaction is proceeding even at room temperature and is almost completed within a few minutes. Similar experiments using a larger amount of water (not shown) resulted in a quantitative conversion of **I** into **II** within 5 min.

Discussion

Two new zinc phosphates, $[(C_5NH_5)(C_4N_2H_{10})][Zn(H_2PO_4)_2(HPO_4)]$, **I**, and $[(C_5NH_5)(C_4N_2H_{10})][Zn_2(H_2PO_4)(HPO_4)(PO_4)]\cdot 2H_2O$, **II**, have been obtained as good quality single crystals, and their structures were determined by single-crystal X-ray diffraction. While **I** has only single four-membered rings made from $Zn_2P_2O_4$ units with hanging phosphate groups from the Zn centers, **II** contains the S4R units with the hanging phosphate groups connected through a Zn atom giving rise to an extended two-dimensional layered structure. As expected, both structures are formed from the tetrahedral building blocks of ZnO_4 and PO_4 units, sharing vertexes, with linkages arising from Zn−O−P bonds. The PO_4 groups are variably protonated to compensate for the charge neutrality of the solids.

A careful examination of the structures of **I** and **II** clearly shows that they are related. It is important to compare the structures of **I** and **II**, and to ponder over the formation of

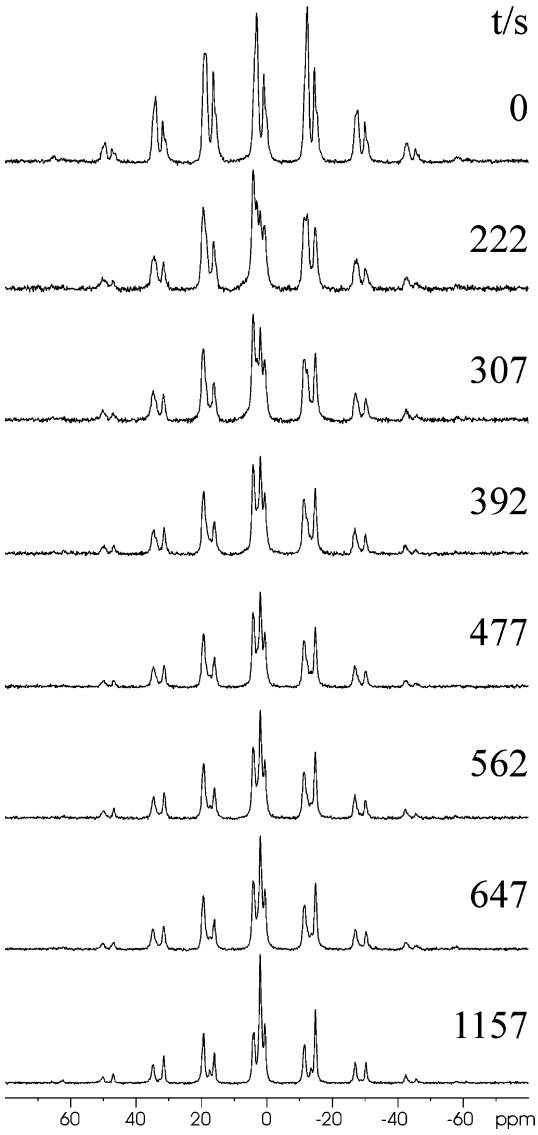

Figure 4. ^{31}P CMAS in situ NMR experiments on the transformation of **I** into **II**. The top spectrum is that of the monomer defining the time zero of the reaction. Consecutive spectra were acquired at the times indicated (t = start time plus 1/2 acquisition time).

such architectures. While the formation of the S4R itself is very rare, the direct condensation of **I** to give rise to **II** is unprecedented. The transformation of **I** to **II** can be understood in terms of a simple reaction:

$$[(C_5NH_5)(C_4N_2H_{10})][Zn(H_2PO_4)_2(HPO_4)] + Zn(OOCCH_3)_2{\cdot}2H_2O \rightarrow [(C_5NH_5)(C_4N_2H_{10})] \times [Zn_2(H_2PO_4)(HPO_4)(PO_4)]{\cdot}2H_2O + 2CH_3COOH$$

It is likely that the acetate anions, formed during the dissolution of the zinc acetate, deprotonated the terminal P−OH group giving rise to the [(P−O)$^-$] species, which readily reacted with the Zn^{2+} ions giving rise to **II**. Acetic acid, formed during the above reaction, is a weak acid and did not give rise to changes in the pH during and after the reaction.

In-situ experimental investigations on the reactivity of lower dimensional solids or the formation of open-framework solids have been rather limited. In-situ X-ray studies have been performed[13,17] and revealed new types of intermediate phases in the formation of three-dimensional open-framework structures. Toulelle et al.[18] studied the synthesis of the aluminophosphate $AlPO_4$–CJ2 using in-situ solution NMR and interpreted the results in terms of a condensation of S4R units into a solid network. In addition, in-situ solid-state MAS NMR has been successfully applied to follow the synthesis of framework solids.[19] In the present study, we have employed the latter approach to study the transformation of the S4R units into an extended structure.

In comparison of the ^{31}P CPMAS spectra of **I** and **II**, a rather strong resemblance is obvious. The signal at approximately 0.7 ppm is found in both samples; the values for the anisotropy parameter Δ_{CS} are similar (Table 5). The local geometries, therefore, of the phosphorus atoms responsible for these two signals (P−O bond lengths and angles) are not very different from one another. The same holds true for the signals at 3.9 ppm in the spectra of **I** and **II**. In this case, the CSA tensors for the two resonances are virtually identical. The obvious difference in the ^{31}P MAS NMR spectra of the monomer (**I**) and the layered zinc phosphate (**II**) is the disappearance of the signal at 3.1 ppm (**I**) and the appearance of a signal at 2.1 ppm (**II**).

A somewhat tentative, yet consistent, assignment of the individual signals is possible by correlating the local geometries of the individual phosphate species in **I** and **II** to the observed CSA tensors of the individual NMR signals. According to the single-crystal structure data there are two H_2PO_4 (P2 and P3) and one HPO_4 unit (P1) in the structure of **I**. In the structure of **II**, P1 constitutes a HPO_4 unit, P2 a PO_4 group, and P3 a H_2PO_4 group. Since the signal at 2.1 ppm is only present in the spectrum of **II**, we can assign this signal to P2(**II**), the PO_4 group. This assignment is supported by the fact, that the P2(**II**) species is the most symmetric species present in the structures of **I** and **II**, which is mirrored in the smallest CSA tensor (cf. Table 5). Next, we ascribe the two H_2PO_4 species in **I** to the signals at 3.9 and 3.1 ppm, respectively. Accordingly, the signal at 0.7 ppm in the spectrum of **I** has to be assigned to P1, the HPO_4 unit.

In a comparison of the local geometries of the various PO_4 tetrahedra in the structures of **I** and **II**, we find very similar P−O bond lengths and angles for P1(**I**) and P1(**II**) as well as for P2(**I**) and P3(**II**). This similarity entails a strong resemblence of the corresponding CSA values. Consequently, considering the strong resemblance of the CSA values for the signals at 0.7 ppm as well as for the signals at 3.9 ppm in the spectra of **I** and **II**, the signal at 0.7 ppm in the spectrum of **II** is assigned to P1(**II**), the HPO_4 unit, and the signal at 3.9 ppm in the spectrum of **II** is assigned to P3(**II**), the H_2PO_4 unit.

(17) Vistad, B.; Akporiaye, D. E.; Lillerud, K. P. *J. Phys. Chem. B* **2001**, *105*, 12437.
(18) Toulelle, F.; Haouas, M.; Geradin, C.; Estournes, C.; Loiseau, T.; Ferey, G. *Colloids Surf., A* **1999**, *158*, 299.
(19) (a) Shi, J. M.; Anderson, M. W.; Carr, S. W. *Chem. Mater.* **1996**, *8*, 369. (b) Vistad, O. B.; Akporiaye, D. E.; Taulelle, F.; Lillerud, K. P. *Chem. Mater.* **2003**, *15*, 1639.

The considerable similarity of the CSA tensors for two of the three phosphorus atoms in **I** and **II** as described above is a strong argument in favor of the conservation of the S4R unit (**I**) during the reaction into the extended structure of **II**, but breaking and reassembly of the S4R can also not be completely ruled out. To elucidate and investigate this point in greater detail, the in-situ ^{31}P CPMAS NMR experiments have been performed. Since the spectra had to be acquired within a short time to obtain a reasonable time resolution, the S/N ratio of the spectra is naturally only limited, thus impeding the complete deconvolution into the spinning sideband patterns. In this respect, the results of the deconvolution of the spectra are not to be taken as the only possible solution as other fits might also prove equally reasonable.

Nevertheless, two important points may be immediately concluded from the in-situ study (Figure 4). First, the phosphorus atoms responsible for the signals at 0.7 ppm obviously do not alter their local environment. Furthermore, the relative area of this signal does not change in the course of the reaction and remains approximately at 0.33. The same holds true for the signal at 3.9 ppm, although here a deconvolution was not possible due to the overlap of the signals. Second, immediately after H_2O addition, two new signals can be observed. The signal at 4.3 ppm exhibits its maximum intensity at short reaction times and is then slowly decaying, whereas the new signal at 2.1 ppm is gradually increasing in intensity.

Since the CPMAS NMR experiment filters out any ^{31}P signals arising from liquid components, we traced the transformation of **I** into **II** using ^{31}P-MAS NMR with high power proton decoupling (not shown). Except for a small additional resonance at 0.34 ppm amounting to ca. 3% of the total intensity, the spectra were identical to the corresponding CPMAS spectra, confirming that no extended liquid phosphate species are present during the conversion of **I** into **II**.

The above observations enable us to propose the following reaction mechanism for the conversion of **I** into **II**. At the center of our discussion is the postulate that the S4R unit is not disassembled during the transformation. The fragment in the structure of **II** resembling the S4R unit of the monomer contains the ring Zn1−P1−Zn1−P1. The conversion of **I** into **II** is not accompanied with extended bending or twisting of the S4R; P3(**I**) is transformed into P2(**II**), P2(**I**) into P3(**II**), and P1(**I**) into P1(**II**), in accordance with the assignment of the ^{31}P NMR signals. The transformations of P1(**I**) into P1(**II**) and of P2(**I**) into P3(**II**) only involve minor changes in the local geometry; therefore, the CSA tensor shows only small variations.

The transformation of P3(**I**) into P2(**II**), however, is accompanied by major changes in the local geometry. Consequently, the ^{31}P NMR signal of P3(**I**) disappears during the transformation of **I** into **II**, being successively replaced by the emerging signal at 2.1 ppm, assigned to P2(**II**). As can be concluded from the appearance and disappearance of the signal at 4.3 ppm, this transformation proceeds in two steps. In Figure 5 the relative areas of all observed signals is plotted as a function of the reaction time. From this, it is obvious that the reaction is a series reaction. P3(**I**) is first transferred into an intermediate (presumably due to the attachment of the first zinc cation). In a second step, the intermediate is transformed into the final product, P2(**II**). For P1(**I**) and P2(**I**), only minor changes in the local geometry are necessary to fit within the extended structure of **II**. In light of the above sequence of reactions, it is important to note that both **I** and **II** have been obtained as pure single-phase materials. The crystallization of **II** from **I** also indicates that the S4R zinc phosphate is reactive and the chemical system is alive.

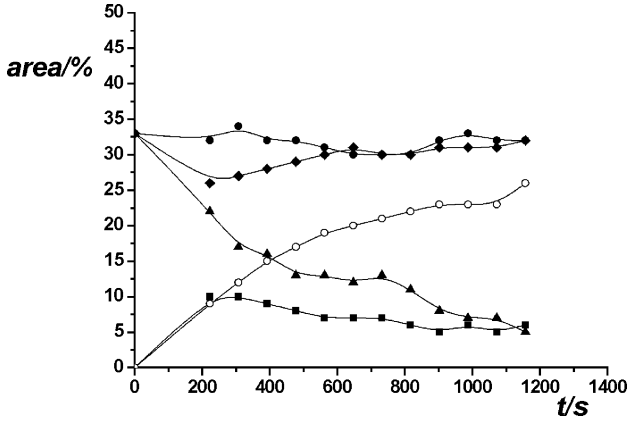

Figure 5. Evolution of the areas of the different ^{31}P signals as a function of the reaction time. For the reaction, a small amount of H_2O was added to an equimolar mixture of **I** and zinc acetate. Consecutive spectra were acquired within 85 s each, the first acquistion starting 2 min after H_2O addition. Key: filled circles, ^{31}P NMR signal at 3.9 ppm; filled diamonds, ^{31}P NMR signal at 0.7 ppm; filled triangles, ^{31}P NMR signal at 3.1 ppm; open circles, ^{31}P NMR signal at 2.1 ppm; filled squares, ^{31}P NMR signal at 4.3 ppm.

A careful examination of the crystallographic lattice parameters of **I** and **II** also reveals close relationships. Both **I** and **II** have identical symmetry with small differences in the cell parameters. While there is a reduction of ∼2 Å in the *c* axis, there is an increase of ∼0.5 and ∼1.6 Å in the *a* and *b* parameters, respectively. These variations in the parameters can be accounted for by the removal of protons from the P−OH linkages (∼0.9 Å) and addition of Zn atoms in **I** to give rise to **II**.

Strong hydrogen bond interactions between the amine molecules and the framework exist in both phosphates (average D···A = ∼2.2 Å and D−H···A = ≥150°). In addition, the $\pi-\pi$ interactions involving the pyridyl molecule of the amine are also important. In Figure 6 we show the two separate fragments of the four-membered rings garnered from the structure of **II** [corresponding to Zn(1) and Zn(2)] along with the structure of **I**. It becomes obvious that the alignment of the amine molecules in pairs plays a subtle role. The amine molecules are aligned trans to each other in the *bc* and the *ac* planes, for **I** and **II**, respectively, and appear to have strong $\pi-\pi$ interactions (average $d_{\text{centroid}-\text{centroid}}$ = 3.5 Å) (Figure 6). This is a typical value and is comparable to those observed in many of the organic supramolecular assemblies involving similar $\pi-\pi$ interactions.[7] It is likely that the organization of the amine molecule has also played a subtle role in the stabilization and reaction of the S4R zinc phosphate.

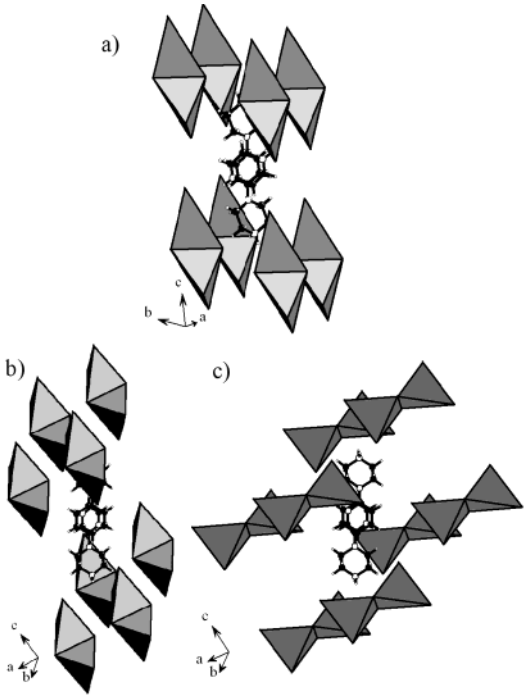

Figure 6. Arrangement of the Py-Pip molecule along the S4R unit in (a) in **I** and (b, c) in **II** showing Zn(1) and Zn(2), respectively. For clarity, S4Rs are drawn as two edge-sharing ZnP_4 tetrahedra. Note the $\pi-\pi$ stacking dimers of the organic amine (see text).

Conclusions

In conclusion, new zinc phosphate **I** consisting of only the single four rings (S4R) has been synthesized, under hydrothermal conditions, and is shown to react with Zn^{2+} ions to give rise to **II**, an open-framework zinc phosphate with a layer structure. What is specially noteworthy is that the structural integrity of the S4Rs has been maintained during the formation of **II** from **I**, as Zn^{2+} ions just add on to the S4Rs. Donor−acceptor hydrogen bond interactions and $\pi-\pi$ interactions involving the pyridyl groups appear to play a subtle role in both phosphates. In-situ ^{31}P MAS NMR investigations on the equimolar mixture of **I** and Zn acetate also indicate that the transformation of **I** to **II** is facile and fast. This study, the first attempt of this kind, clearly demonstrates that it is possible to combine the principles of organic supramolecular assembly and inorganic building blocks in the formation of new solids with extended architectures.

Acknowledgment. S.N. thanks Prof. C. N. R. Rao, FRS, for his support. S.N. also thanks the Department of Science and Technology (DST), Government of India, for the award of a research grant and gratefully acknowledges the Royal Society of Chemistry for the travel support under the Travel Grant for International Authors program and the Max-Planck-Gesellschaft for financial support.

Supporting Information Available: Tables of atomic coordinates and isotropic thermal parameters of the non-hydrogen atoms, experimental and simulated powder X-ray patterns of **I** and **II**, ORTEP plots of **I** and **II**, and crystallographic data in CIF format for **I** and **II**. This material is available free of charge via the Internet at http://pubs.acs.org.

IC0301831